Theor Chem Acc (2010) 125:57–64
DOI 10.1007/s00214-009-0659-0

REGULAR ARTICLE

Theoretical studies of decomposition kinetics of CF_3CCl_2O radical

Hari Ji Singh · Bhupesh Kumar Mishra · Nand Kishor Gour

Received: 4 August 2009 / Accepted: 6 October 2009 / Published online: 29 October 2009

Abstract The unimolecular decomposition reaction of CF_3CCl_2O radical has been investigated using theoretical methods. Two most important channels of decomposition occurring via C–C bond scission and Cl elimination have been considered during the present investigation. Ab initio quantum mechanical calculations are performed to get optimized structure and vibrational frequencies at DFT and MP2 levels of theory. Energetics are further refined by the application of a modified Gaussian-2 method, G2M(CC,MP2). The thermal rate constants for the decomposition reactions involved are evaluated using Canonical Transition State Theory (CTST) utilizing the ab initio data. Rate constants for C–C bond scission and Cl elimination are found to be 6.7×10^6 and 1.1×10^8 s^{-1}, respectively, at 298 K and 1 atm pressure with an energy barrier of 8.6 and 6.5 kcal/mol, respectively. These values suggest that Cl elimination is the dominant process during the decomposition of the CF_3CCl_2O radical. Transition states are searched on the potential energy surface of the decomposition reactions involved and are characterized by the existence of only one imaginary frequency (NIMAG = 1) during frequency calculation. The existence of transition states on the corresponding potential energy surface is further ascertained by performing intrinsic reaction coordinate (IRC) calculation.

Keywords Theoretical chemistry · Haloalkoxy radicals · Decomposition of HCFC-123 · Canonical transition state theory

H. J. Singh (✉) · B. K. Mishra · N. K. Gour
Department of Chemistry, DDU Gorakhpur University, Gorakhpur, Uttar Pradesh 273009, India
e-mail: hari_singh81@hotmail.com

1 Introduction

Reasonably acceptable chemical and physical properties along with their thermodynamic and transport properties rendered CFCs suitable for a variety of industrial applications. Most of the CFCs have excellent chemical and physical properties, such as stability, nonreactivity, nontoxicity and nonflammability, very well suited for a variety of industrial applications. They usually possess high densities and low boiling points, viscosities and surfaces tensions. The very stability of fully halogenated CFCs that makes them so useful also renders them dangerous to the stratospheric ozone layer. Chlorine radicals generated by the decomposition of CFCs in the stratosphere through a series of catalytic reactions lead to a net decrease in the total ozone concentration in the upper atmosphere leading to an increase in the earth's temperature (the "greenhouse effect") [1–4]. Ozone-layer depletion increases the amount of damaging ultraviolet radiation that penetrates to the earth's surface. The threat of CFCs to the ozone layer was considered so serious that an international treaty, the 1987 Montréal Protocol, was developed to prohibit production and use of CFCs and most other chemicals causing ozone depletion.

The phasing out of CFCs has created an urgent need for acceptable substitutes. Attention has been focused on the synthesis of hydrofluorocarbons (HFCs) and hydrochlorofluorocarbons (HCFCs) for replacing CFCs in refrigeration and air-conditioning systems [5, 6]. The choice of using HFCs and HCFCs instead of CFCs is motivated by a number of factors. HFCs do not contain Cl atoms and therefore do not have any ozone depletion potential associated with the well-established chlorine catalytic cycle [7]. On the other hand, HCFCs do contain Cl atoms; however, the delivery of the Cl atoms from these compounds is inefficient since most of the HCFCs are scavenged by OH

radical in the troposphere. HFCs and HCFCs contain one or more C–H bonds that make them susceptible to attack by OH radicals in the troposphere initiating its tropospheric decomposition [8].

One of the most widely used HCFCs is 2,2-dichloro-1,1,1-trifluoroethane (HCFC-123). HCFC-123 is a synthetic, non-combustible volatile liquid that is used as a refrigerant in commercial and industrial air-conditioning installations as an alternative to trichlorofluoromethane (CFC-11) and dichlorofluoromethane (CFC-12). It is also widely used as a gaseous fire extinguisher, and also as a metal and electronics cleaning agent. Although HCFC-123 contains chlorine, its hydrogen-containing molecule decomposes primarily in the lower atmosphere before it can reach the ozone layer. Because the chlorine is dissipated at lower altitudes, HCFCs have relatively short atmospheric lifetimes and much lower ozone depletion potentials (ODPs) than CFCs. The estimated atmospheric lifetime of HCFC-123 is 1.4 years [9]. Its ozone-depleting potential is 0.02 relative to CFC-11 (trichlorofluoromethane) [9]. It has a global warming potential of 300 over a 20-year time horizon relative to carbon dioxide. As such, HCFC-123 is currently used as a transitional replacement for chlorofluorocarbons and bromofluorocarbons phased out in pursuant to 1987 Montreal Protocol on substances that deplete the ozone layer. HCFC-123 is degraded into the atmosphere by reaction with photochemically produced hydroxyl radicals [10]. This is the dominant path for removing these compounds from the troposphere (Scheme 1). A general mechanism of tropospheric degradation mechanism of HCFC-123 may be shown as follows.

The above scheme is based on the fact that the initial attack of OH radical on HCFC-123 leads to the formation of haloalkyl radicals ($CF_3CCl_2^{\bullet}$), which in turn reacts with atmospheric O_2 to give peroxy radicals, $CF_3CCl_2O_2^{\bullet}$ [11]. The latter react further with NO leading to the formation of haloalkoxy radicals, $CF_3CCl_2O^{\bullet}$ via a short-lived intermediate, the peroxynitrate ($CF_3CCl_2O_2NO_2$). On the other hand, haloalkoxy radical may also be generated through another intermediate, the hydroperoxide ($CF_3CCl_2O_2H$) formed by the reaction of $CF_3CCl_2O_2$ and HO_2 radicals. The haloalkoxy radicals thus formed from HCFC-123 in the atmosphere play an important role in the degradation mechanism of organic vapors in the troposphere [12, 13]. During the recent past, considerable theoretical studies have been performed on other similar haloalkoxy radicals [14–18].

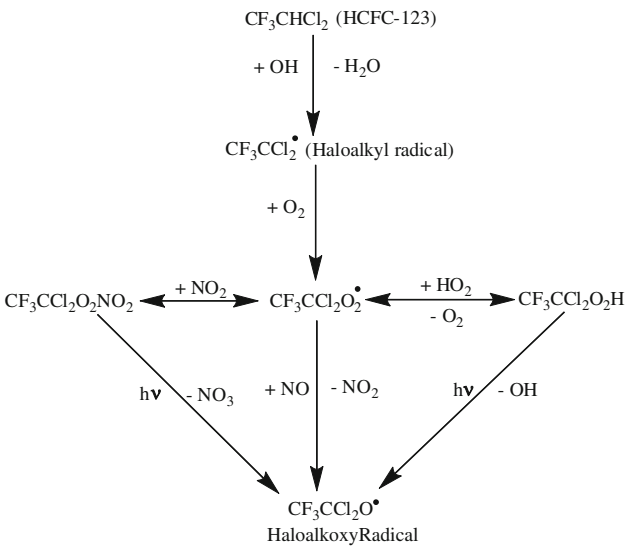

Scheme 1 Tropospheric degradation mechanism of HCFC-123

In this study, we present a theoretical study of the thermal decomposition of CF_3CCl_2O radical using high-level ab initio molecular orbital methods. We confined ourselves to the investigation of the two potential decomposition channels, viz., C–C bond scission and Cl elimination as given below:

$$CF_3CCl_2O \rightarrow CF_3 + C(O)Cl_2 \quad (1)$$

$$\rightarrow CF_3C(O)Cl + Cl. \quad (2)$$

Literature survey reveals that there is very little information available in literature and, to the best of our knowledge, no experimental data are available on this important radical that could play a critical role in the destruction of many other organic vapors placed into the atmosphere by anthropogenic or industrial means. This motivated us to investigate the reaction channels (reactions 1 and 2) on a sound theoretical basis. We carried out detailed ab initio calculations to elucidate the mechanism of thermal decomposition of this important haloalkoxy radical. We also tried to calculate rate constants for the decomposition channels using canonical transition state theory.

2 Computational method

Ab initio calculations [19] performed during the course of the present investigation were done using the GAUSSIAN 03 series of program [20]. Geometries of all the reactants, products, intermediates and transition states for reactions (1) and (2) were optimized at the B3LYP/6-311G(d,p) and MP2/6-311G(d,p) levels. We used one of the hybrid models, namely Becke's three parameter non-local exchange functional [21] B3LYP. The correlation functional for this model is that proposed by Lee, Yang and Parr [22] for a non-local approximation. Vibrational frequencies employed for characterization of stationary points, zero-point energies (ZPE) corrections, and rate

constants calculations were also computed at the DFT-B3LYP level of theory. All the stationary states were identified for the local minima. All the vibrational frequencies for stable products were identified with a positive value (NIMAG = 0). On the other hand, transition states were characterized by the occurrence of only one imaginary frequency (NIMAG = 1). To confirm that the transition state connected smoothly to the reactant and products, intrinsic reaction coordinate (IRC) calculations [23] were also performed with the same level of theory at which optimization and frequency calculation were performed.

To obtain more reliable energies of various species, a variant of the Gaussian-2 (G2) type methodology [24] has been used during the present study. Mebel et al. [25] have recommended the G2M(CC,MP2) version for the system that contains six or seven heavy atoms.

According to the proposed scheme, the geometry and frequency are performed at B3LYP/6-311G(d,p) level and single point energy calculation is done at MP2 and MP4 levels. A CCSD(T)/6-311G(d,p) calculation is substituted for the QCISD(T)/6-311G(d,p) calculation of the original G2 method. The additivity scheme of modified G2 composite method such as G2M(CC,MP2) yields a composite energy calculation briefly described as follows:

$$\mathrm{E[G2M(CC,MP2)]} = \mathrm{E_{base}} + \Delta\mathrm{E(3df,2p)} + \Delta\mathrm{E(CC)} + \mathrm{HLC} + \mathrm{ZPE}$$

where

E_{base} = E[MP4/6-311G(d,p)],
ΔE(3df, 2p) = E[MP2/6-311 + G(3df,2p)] − E[MP2/6-311G(d,p)],
ΔE(CC) = E[CCSD(T)/6-311G(d,p)] − E[MP4/6-311G(d,p)],
HLC = $-0.00525\mathrm{n}_{\alpha} - 0.00019\mathrm{n}_{\beta}$ is the high-level correction, and
ZPE = zero-point energy

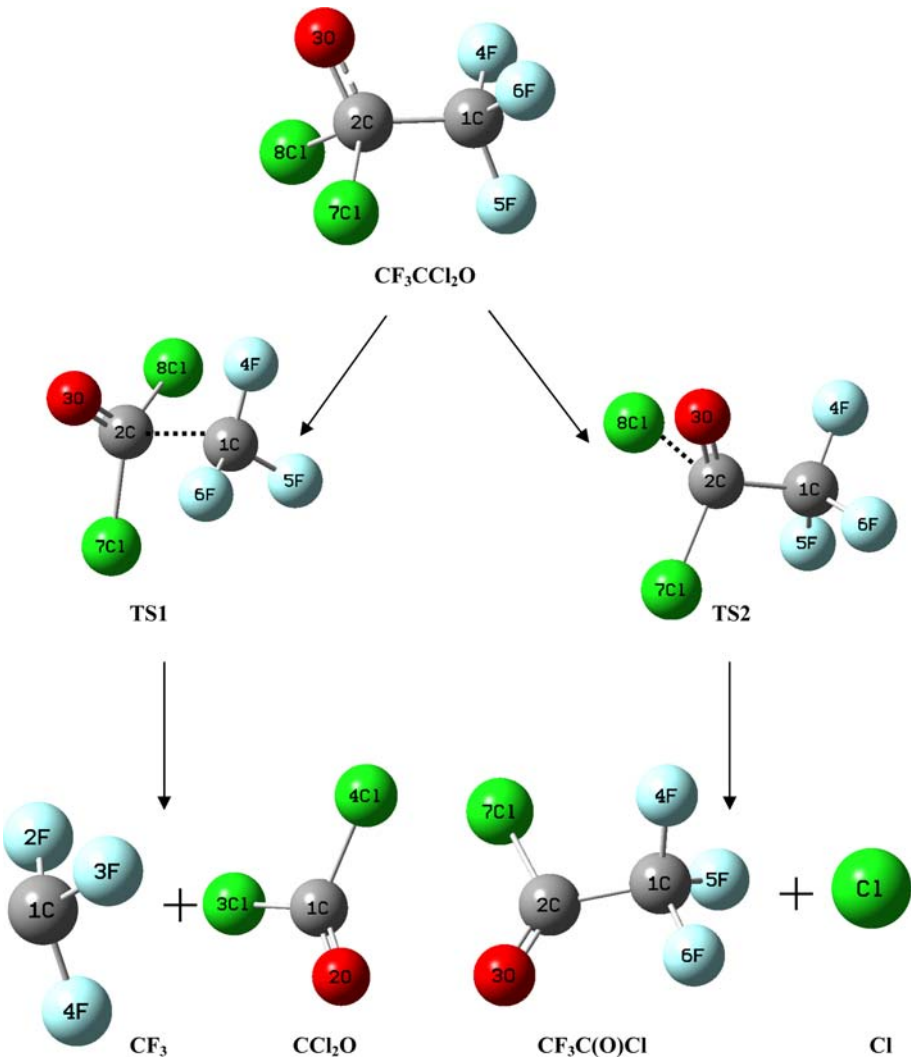

Fig. 1 Optimized geometries of reactant, products and transition states involved in the decomposition of CF_3CCl_2O using the B3LYP/6-311G(d,p) method

Table 1 Structural parameters of reactants, products and transition states involved in CF_3CCl_2O decomposition at the B3LYP/6-311G(d,p) (first line) and MP2/6-311G(d,p) (second line) levels of theory

	CF_3CCl_2O	TS1	TS2	CF_3	CCl_2O	$CF_3C(O)Cl$
Bond length (Å)						
R (C1–C2)	1.567	1.997	1.491	–	–	1.555
	1.547	1.917	1.553	–	–	1.544
R (C1–F4)	1.334	1.308	1.331	–	–	1.337
	1.328	1.300	1.332	–	–	1.332
R (C1–F5)	1.333	1.309	1.340	–	–	1.330
	1.328	1.304	1.325	–	–	1.325
R (C1–F6)	1.337	1.308	1.330	–	–	1.337
	1.332	1.300	1.334	–	–	1.332
R (C2–O3)	1.308	1.204	1.250	–	–	1.177
	1.352	1.193	1.225	–	–	1.189
R (C1–O2)	–	–	–	–	1.171	–
	–	–	–	–	1.182	–
R (C2–Cl7)	1.810	1.825	1.788	–	–	1.782
	1.770	1.792	1.750	–	–	1.750
R (C2–Cl8)	1.844	1.825	2.076	–	–	–
	1.771	1.792	2.076	–	–	–
R (C1–Cl3)	–	–	–	–	1.770	–
	–	–	–	–	1.747	
R (C1–F2)	–	–	–	1.323	–	–
	–	–	–	1.317	–	–
R (C1–F3)	–	–	–	1.323	–	–
	–	–	–	1.317	–	–
R (C1–F4)	–	–	–	1.323	–	–
	–	–	–	–	1.317	–
Bond angle (deg)						
A (F2–C1–F3)	–	–	–	111.227	–	–
	–	–	–	111.348		–
A (F2–C1–F4)	–	–	–	111.227	–	–
	–	–	–	111.348	–	–
A (F4–C1–F5)	108.890	112.134	108.834	–	–	108.973
	108.926	111.948	109.547	–	–	109.025
A (F4–C1–F6)	108.445	112.116	109.357	–	–	108.801
	108.383	112.430	108.786	–	–	108.816
A (F5–C1–F6)	109.010	112.134	108.579	–	–	108.973
	109.056	111.948	108.871	–	–	109.025
A (C1–C2–Cl7)	109.197	100.104	111.113	–	–	112.284
	109.196	100.067	111.396	–	–	112.027
A (C1–C2–Cl8)	108.931	100.104	104.143	–	–	–
	109.673	100.067	102.571	–	–	–
A (O3–C2–Cl7)	113.914	120.735	118.920	–	–	123.805
	111.969	121.342	121.115	–	–	124.383
A (O3–C2–Cl8)	99.388	120.735	92.019	–	–	–
	102.930	121.342	88.687	–	–	–
A (Cl7–C2–Cl8)	110.670	109.454	107.924	–	–	–
	111.962	109.792	107.377	–	–	–

Table 1 continued

	CF_3CCl_2O	TS1	TS2	CF_3	CCl_2O	$CF_3C(O)Cl$
A (Cl3–C1–Cl4)	–	–	–	–	112.027	–
	–	–	–	–	112.238	–
A (Cl3–C1–O2)	–	–	–	–	123.997	–
	–	–	–	–	123.880	–

Table 2 Unscaled vibrational frequencies of reactants, products and transition states in CF_3CCl_2O decomposition at the B3LYP/6-311G(d,p) (first line) and MP2/6-311G(d,p) (second line) levels of theory

Species	Vibrational frequencies (cm^{-1})
CF_3CCl_2O	65, 172, 191, 240, 275, 310, 356, 478, 531, 583, 657, 727, 874, 1,164, 1,208, 1,226, 1,242, 3,170
	79, 187, 207, 300, 316, 375, 840, 410, 510, 569, 602, 747, 862, 947, 1,153, 1,266, 1,282, 1,328
TS1	298i, 57, 135, 160, 221, 240, 292, 385, 395, 491, 534, 545, 705, 715, 998, 1,301, 1,308, 1,566
	849i, 80, 155, 182, 250, 278, 310, 381, 429, 536, 556, 577, 726, 812, 974, 1,349, 1,370, 1,546
TS2	349i, 63, 151, 183, 219, 301, 325, 382, 431, 493, 569, 582, 732, 892, 1,187, 1,215, 1,238, 1,382
	880i, 77, 162, 194, 234, 308, 344, 408, 415, 523, 573, 601, 760, 955, 1,243, 1,280, 1,299, 1,435
CF_3	504, 540, 692, 1,077, 1,242, 1,243
	520, 520, 716, 1,123, 1,301, 1,301
CCl_2O	300, 435, 549, 581, 802, 1,900
	319, 457, 584, 597, 866, 1,851
CF_3C (O) Cl	35, 193, 230, 332, 394, 497, 507, 577, 703, 737, 910, 1,191, 1,227, 1,254, 1,902
	45, 203, 238, 346, 408, 520, 526, 595, 712, 759, 951, 1,243, 1,284, 1,320, 1,844

In the high-level correction (HLC), n_α and n_β are the number of α and β valence electrons, respectively, with $n_\alpha \geq n_\beta$. The zero-point energy is obtained from harmonic vibrational frequency calculation performed at B3LYP/6-311 G(d,p) level.

3 Results and discussion

The fate of haloalkoxy radical (CF_3CCl_2O) considered during the course of the present investigation is predominantly its thermal decomposition in the atmosphere. Two dominant decomposition pathways considered via reactions 1 and 2 involve transition states TS1 and TS2, respectively. Optimized geometries of reactant, products and transition states are performed at B3LYP/6-311G(d,p) and MP2/6-311G(d,p) level of theories. Results obtained at MP2 level are shown in Fig. 1. Geometrical parameters obtained at both levels are recorded in Table 1. The results show that structural parameters are remarkably close and are in very good agreement with each other. To check the influence of the basis set, the 6-311++G(d,p) basis set is employed with the same method to reoptimize the geometries of the reactant and transition states involved. It is observed that the geometrical parameters are in reasonable agreement with those obtained at the 6-311G(d,p) level. Therefore, it may be concluded that addition of multiple diffuse functions has no significant effect on the energetics of the decomposition channels of the title compound. The results obtained during frequency calculations for reactant, products and transition states using both methods are recorded in Table 2. Results show that values obtained using MP2 method is slightly higher than that of DFT (B3LYP). These results also show that the reactant and products have stable minima on their potential energy surface and these are characterized by the occurrence of real vibrational frequencies. Results recorded in Table 2 show the occurrence of only one imaginary frequency at 298 and 349 cm^{-1} for TS1 and TS2, respectively at the B3LYP level, whereas the corresponding values at MP2 are 849 and 880 cm^{-1}. These frequencies are analyzed using the GaussView program [26]. Visualization of vibrations corresponding to the calculated imaginary frequencies show the well-defined transition state geometries connecting reactant and products. To ascertain the existence of transition state on the corresponding potential

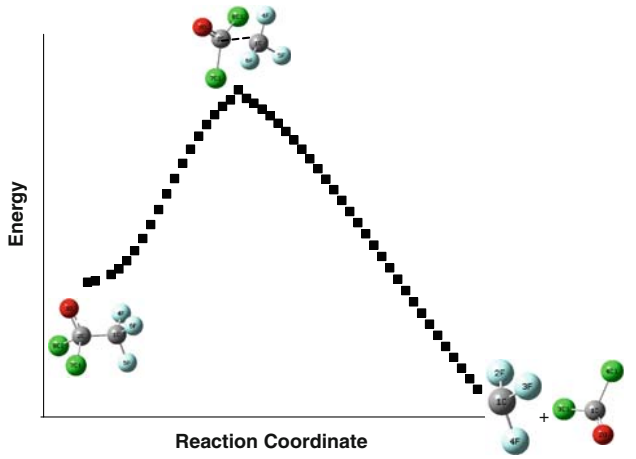

Fig. 2 IRC plot for the transition state TS1 for C–C bond scission in the CF_3CCl_2O decomposition in the B3LYP/6-311G(d,p) method. The reactant, transition state and products are also shown along the reaction path

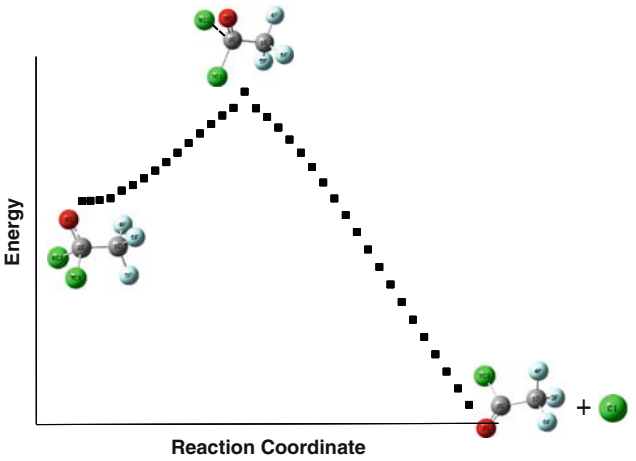

Fig. 3 IRC plot for the transition state TS2 for Cl elimination in the CF_3CCl_2O decomposition in the B3LYP/6-311G(d,p) method. The reactant, transition state and products are also shown along the reaction path

energy surface, intrinsic reaction path calculations (IRC) are also performed for each transition state. The IRC plots shown in Figs. 2 and 3 reveal the transition state structure moving energetically downhill until the reactant and products are reached as complementary end point of the reaction path. Visualization of the optimized structure of TS1 further reveals the elongation of C–C bond length from 1.567 to 1.997 Å at B3LYP and 1.547 to 1.917 Å at the MP2 level. At the same time, a shrinkage of the C–O distance from 1.308 to 1.204 Å at B3LYP and 1.352 to 1.193 Å at MP2 and formation of a carbon–oxygen double bond has also been observed. These results are in accord with that obtained in an earlier study performed at the same level by Stevens et al. [17] for C–C bond scission in a similar haloalkoxy radical, CF_3CFHO, in which they found an increase of C–C bond distance from 1.567 to 2.038 Å together with a decrease in the C–O bond distance from 1.308 to 1.208 Å in the transition state structure. On the other hand, in another computational study conducted by Somnitz and Zellner [15] on CF_3CF_2O, the elongation of the C–C bond was found to be from 1.592 to 1.980 Å, together with a decrease in C–O bond distance from 1.321 to 1.216 Å. Similar observations have also been observed by Hou et al. [18]. The analysis of TS2 obtained during the present study for the Cl elimination reveals the elongation of C–Cl bond length from 1.844 to 2.076 Å (13%) at B3LYP and 1.771 to 2.076 Å at MP2 (18%). Hou et al. [18] also reported an increase of 18% in the C–Cl distance. The results obtained during the present study further reveals a simultaneous shrinkage of C–O bond distance in TS2 also as recorded in Table 1.

Single point energy calculations of the reactant (CF_3CCl_2O), products (CF_3, $C(O)Cl_2$, $CF_3C(O)Cl$ and Cl) and transition states (TS1 and TS2) are made using MP2 and CCSD(T) methods. Results are recorded in Table 3. In each method, the geometry optimized at B3LYP/6-311G(d,p) level is taken. Calculated total energies are corrected for zero-point energy, the latter being determined at the HF/6-31G(d) level and corrected with a scale factor of 0.8929 [14]. Zero-point corrected total energies using standard and extended basis sets for various species and transition states involved in the present investigation are also recorded in Table 3. To have a more refined energy value for the species involved, G2M(CC,MP2) basis set additivity method is used. These results are also listed in Table 3. Energy barriers for C–C bond scission and Cl elimination channels occurring via TS1 and TS2, respectively, are evaluated from the zero-point energy corrected total energies, as recorded in Table 3, and values are recorded in Table 4. Table 4 also lists the energy barriers for C–C bond scission computed by Wu and Carr [16] at various levels of theory for a similar haloalkoxy radical, CF_3CFHO. The data reveal a comparable value of energy barriers for C–C bond scission. It is observed that energy barrier decreases as the basis set is extended. Using the most acclaimed procedure for calculating barrier height for such molecules, the G2M(CC,MP2) method [27] yields a value of 8.6 and 6.5 kcal mol^{-1} for C–C bond scission and Cl elimination process. This corroborates the dominance of Cl elimination pathways in the decomposition process of CF_3CCl_2O radical. An extensive literature survey reveals the absence of any experimental or theoretical data available for making a comparison of these values. However, an intensive ab initio calculation performed by Somnitz and Zellner [15] for a similar species CF_3CF_2O yielded a value of 8.1 kcal mol^{-1} for C–C bond scission. The G2(MP2) calculation of Wu and Carr [16] found a value of 9.5 kcal mol^{-1} for C–C bond scission in another similar

Table 3 Zero-point energy corrected total energies for species involved in CF_3CCl_2O decomposition (unit: hartree)

Level	CF_3CCl_2O	TS1	TS2	$CF_3 + C(O)Cl_2$	$CF_3C(O)Cl + Cl$
MP2/6-311G(d, p)	−1,369.267110	−1,369.246917	−1,369.249890	−1,369.235237	−1,369.298388
MP2/6-311+G(3df, 2p)	−1,369.649962	−1,369.632114	−1,369.637079	−1,369.616426	−1,369.672768
MP4/6-311G(d, p)	−1,369.351468	−1,369.332581	−1,369.341570	−1,369.362291	−1,369.37921
MP4/6-311G(2df, 2p)	−1,369.707297	−1,369.690997	−1,369.698282	−1,369.717133	−1,369.730443
MP4/6-311++G(2df, 2p)	−1,369.729723	−1,369.713075	−1,369.720654	−1,369.740157	−1,369.751626
CCSD(T)/6-311++G(d,p)	−1,369.346670	−1,369.332135	−1,369.340314	−1,369.351947	−1,369.368503
G2M(CC,MP2)	−1,369.953377	−1,369.939575	−1,369.942969	−1,369.956412	−1,369.966066

Table 4 Calculated energy barriers in kcal mol^{-1}

Method	C–C bond scission	Cl elimination
MP2/6-311G(d,p)	12.6 (14.19)	10.8
MP2/6-311+G(3df,2p)	11.2 (12.61)	8.0
MP4/6-311G(d,p)	11.8 (13.81)	6.2
MP4/6-311G(2df,2p)	10.2 (12.41)	5.6
MP4/6-311++G(2df,2p)	10.4	5.7
CCSD(T)/6-311G(d,p)	9.1	3.9
G2M(CC,MP2)	8.6 (9.5)	6.5

The values in parenthesis are for CF_3CFHO radical [16]

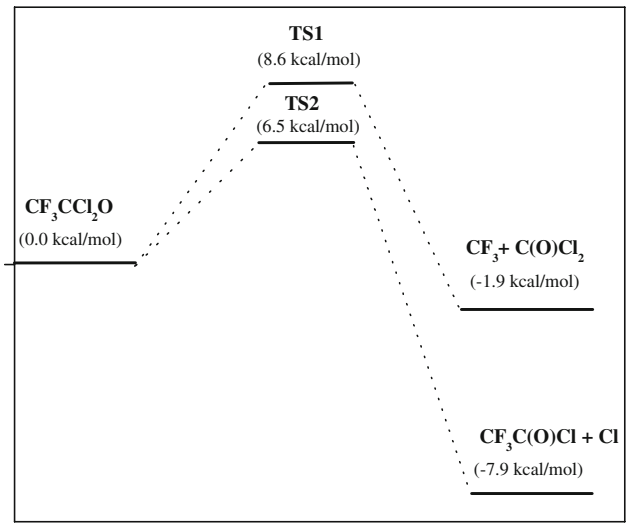

Fig. 4 Relative energy diagram for the thermal decomposition of CF_3CCl_2O at the G2M(CC,MP2) level

compound, CF_3CFHO. Thus, the calculated value of 8.6 kcal mol^{-1} for the C–C bond scission in CF_3CCl_2O obtained during the present study at G2M(CC,MP2) level, as recorded in Table 4, shows good agreement. This gives us a confidence that energy barrier calculated using the G2M(CC,MP2) method on the geometries optimized at B3LYP/6-311G(d,p) yields reliable values for the decomposition channels considered in the present study. An energy diagram constructed with the zero-point corrected energies data relative to the ground state energy of CF_3CCl_2O arbitrarily taken as zero is plotted in Fig. 4. The barrier height of 6.5 kcal/mol for Cl elimination is lower than that of the C–C bond scission. This makes the Cl elimination pathway the dominant process for the dissociation of this haloalkoxy radical in the atmosphere. The dominance of Cl elimination pathway in the thermal decomposition of haloalkoxy radicals has also been confirmed experimentally by Bhatnagar and Carr [27, 28]. Spin contamination is not important for the CF_3CCl_2O radical because $\langle S^2 \rangle$ is in the range of 0.758 at HF/6-31G(d) to 0.76 at MP2/6-311G(d,p) before annihilation. These values are only slightly higher than the expected value of $\langle S^2 \rangle = 0.75$ for doublets.

4 Rate constants

Modeling of the rate constants of decomposition reactions involved is attempted with the Canonical transition state theory (CTST) [29] that includes a semi-classical one-dimensional multiplicative tunneling correction factor. The rate constants are calculated using the following expression:

$$k = \Gamma(T)\frac{k_B T}{h}\frac{Q^{\ddagger}_{TS}}{Q_R}\exp\frac{-\Delta E}{RT} \tag{3}$$

where $\Gamma(T)$ is the tunneling correction factor at temperature T, and $Q^{\ddagger}_{TS}$ and Q_R are the total partition functions for the transition state and reactant, respectively. ΔE, k_B and h have their usual meaning. We adopted the simple and computationally inexpensive Wigner's method [30] for the evaluation of the tunneling correction factor $\Gamma(T)$ as given by the following expression

$$\Gamma(T) = 1 + \frac{1}{24}\left(\frac{h\nu^{\#}}{k_B T}\right)^2 \tag{4}$$

where $\nu^{\#}$ is the imaginary frequency at the saddle point. The tunneling correction factor $\Gamma(T)$ is found to be almost unity. The partition functions for the respective transition

state and reactant at 298 K are obtained from the harmonic vibrational frequencies calculated at the B3LYP/6-311G(d,p) level. The rate constants for C–C bonds scission and Cl elimination in CF_3CCl_2O decomposition involving the transition states, TS1 and TS2, are calculated to be $k_{C-C} = 6.7 \times 10^6\ s^{-1}$ and $k_{C-Cl} = 1.1 \times 10^8\ s^{-1}$ with associated A factor as $A_{C-C} = 1.2 \times 10^{13}\ s^{-1}$ and $A_{C-Cl} = 6.7 \times 10^{12}\ s^{-1}$, respectively, at 298 K and 1 atm pressure. No experimental or theoretical data are available in literature to compare our calculated values. However, Somntiz and Zellner [15] reported rate constant for C–C bond scission for a structurally similar molecule CF_3CF_2O as $k_{C-C} = 5.3 \times 10^6\ s^{-1}$ with the associated A factor as $4.8 \times 10^{13}\ s^{-1}$. The values obtained during the present investigation are in good agreement. Our calculated values show a good correspondence. Thus, we conclude that kinetics parameters for Cl elimination obtained during the present study would also be reasonably accurate.

5 Conclusion

The potential energy surface and reaction mechanism of the thermal decomposition of CF_3CCl_2O radical are investigated at G2M(CC,MP2)//B3LYP/6-311G(d,p) level of theory. Two important channels of decomposition namely C–C bond scission and Cl elimination are considered in detail. The pathways involving Cl elimination is found to be favorable for the CF_3CCl_2O radical decomposition. The critical transition state for this channel, TS2, lies at 6.5 kcal mol^{-1} above CF_3CCl_2O. The barrier height for C–C bond scission involving a transition state TS1 is calculated to 8.6 kcal mol^{-1}, which is in good agreement with the values calculated for other halogenated ethoxy radicals. The thermal rate constants evaluated for the C–C bond scission and Cl elimination decomposition pathway are found to be 6.7×10^6 and $1.1 \times 10^8\ s^{-1}$ at 298 K and 1 atm pressure, respectively, using the conventional transition state theory.

Acknowledgments The authors are thankful to the University Grants Commission, New Delhi for providing fellowships to BKM and NKG under its DSA Program to the Department of Chemistry, DDU Gorakhpur University, Gorakhpur.

References

1. Solomon S (1990) Nature (Lond) 6291:347–354
2. Molina MJ, Rowland FS (1974) Nature 249:810–814
3. Rowland FS, Molina MJ (1994) Chem Eng News 8:72–76
4. Weubbles DJ (1983) J Geophys Res 88:1433–1443
5. Scientific Assessment of Stratospheric Ozone (1989) Vol 11; World Meteorological Organization, Global Ozone Research and Monitoring Project Report No. 20
6. Wayne RP (2001) Chemistry of atmospheres. Clarendon Press, Oxford
7. Ravishankara AR, Lovejoy ER (1994) J Chem Soc Faraday Trans 90:2159–2169
8. Geirczak T, Talukdar R, Vaghjiani GL, Lovejoy ER, Ravishankara AR (1991) J Geophys Res 96(D3):5001–5011
9. Scientific Assessment of Stratospheric Ozone (1995) World Meteorological Organization, Global Ozone Research and Monitoring Project
10. Atkinson R (1990) Atoms Environ Part A 24A:1–41
11. Wallington TJ, Hurley MD, Fracheboud JM, Orlando JJ, Tyndall GS, Sehested J, Mogelberg TE, Nielsen OJ (1996) J Phys Chem 100:18116–18122
12. Brasseur GP, Orlando JJ (1999) Atmospheric chemistry and global change. Oxford University Press, New York
13. Zellner R (1999) Global aspect of atmospheric chemistry. Steinkopff Darmstadt, Germany
14. Fuxiang WU, Carr RW (2002) J Phys Chem A 106:5832–5840
15. Somnitz H, Zellner R (2001) Phys Chem Chem Phys 3:2352–2364
16. Fuxiang WU, Carr RW (2003) J Phys Chem A 107:10733–10742
17. Stevens JE, Jabo Khayat RA, Radkevich O, Brown J (2004) J Phys Chem A 108:11354–11361
18. Hou H, Wang B, Gu Y (2000) J Phys Chem A 104:1570–1575
19. Hehre WJ, Radom L, Schleyer PvR, Pople JA (1986) Ab initio molecular orbital theory. Wiley, New York
20. Frisch MJ, Trucks GW, Schlegel HB, Scuseria GE, Robb MA, Cheeseman JR, Montgomery JA, Jr., Vreven T, Kudin KN, Burant JC, Millam JM, Iyengar SS, Tomasi J, Barone V, Mennucci B, Cossi M, Scalmani G, Rega N, Petersson GA, Nakatsuji H, Hada M, Ehara M, Toyota K, Fukuda R, Hasegawa J, Ishida M, Nakajima T, Honoda Y, Kitao O, Naki H, Klene M, Li X, Knox JE, Hratchian HP, Cross JB, Adamo C, Jaramillo J, Gomperts R, Stratmann RE, Yazyev O, Austin AJ, Cammi R, Pomelli C, Ochterski JW, Ayala PY, Morokuma K, Voth GA, Salvador P, Dannenberg JJ, Zakrzewski VJ, Dapprich S, Daniels AD, Strain MC, Farkas O, Malick DK, Rabuck AD, Raghavachari K, Foresman GB, Ortiz JV, Cui Q, Baboul AG, Clifford S, Cioslowski J, Stefanov BB, Liu G, Liashenko A, Piskorz P, Komaromi I, Martin RL, Fox DJ, Keith T, AL-Laham MA, Peng CY, Nanayakkara A, Challacombe M, Gill PMW, Johnson B, Chen W, Wong MW, Gonzalez C, Pople JA (2004) Gaussian 03; Revision C. 02, Gaussian, Inc, Wallingford
21. Becke AD (1993) J Chem Phys 98:5648–5652
22. Lee C, Yang W, Parr RG (1988) Phys Rev B37:785–789
23. Gonzalez C, Schlegel HB (1990) J Chem Phys 94:5523–5527
24. Curtiss LA, Raghavachari K, Trucks GW, Pople JA (1991) J Chem Phys 94:7221–7230
25. Mebel AM, Morokuma K, Lin MC (1995) J Chem Phys 103:7414–7421
26. Frisch A, Nielsen AB, Holder AJ (2000) Gauss view reference. Gaussian Inc, Wallingford
27. Bhatnagar A, Carr RW (1995) J Phys Chem 99:17573–17577
28. Bhatnagar A, Carr RW (1996) Chem Phys Lett 258:651–656
29. Truhlar DG, Garrett BC, Klippenstein SJ (1996) J Phys Chem 100:12771–12800
30. Wigner EP (1932) Z Phys Chem B19:203–216